Hindawi
Complexity
Volume 2022, Article ID 8437910, 17 pages
https://doi.org/10.1155/2022/8437910

Research Article

A Type-3 Fuzzy Approach for Stabilization and Synchronization of Chaotic Systems: Applicable for Financial and Physical Chaotic Systems

Man-Wen Tian,[1] Yassine Bouteraa,[2] Khalid A. Alattas,[3] Shu-Rong Yan,[1] Abdullah K. Alanazi,[4] Ardashir Mohammadzadeh ,[5] and Saleh Mobayen [6]

[1]*National Key Project Laboratory, Jiangxi University of Engineering, Xinyu 338000, China*
[2]*Robotics and Artificial Intelligence Laboratory (RAILab), College of Computer Engineering and Sciences, Prince Sattam Bin Abdulaziz University, Al-Kharj 11942, Saudi Arabia*
[3]*Department of Computer Science and Artificial Intelligence, College of Computer Science and Engineering, University of Jeddah, Jeddah, Saudi Arabia*
[4]*Department of Chemistry, Faculty of Science, Taif University, P.O. Box 11099, Taif 21944, Saudi Arabia*
[5]*Multidisciplinary Center for Infrastructure Engineering, Shenyang University of Technology, Shenyang 110870, China*
[6]*Future Technology Research Center, National Yunlin University of Science and Technology, Douliu 64002, Taiwan*

Correspondence should be addressed to Ardashir Mohammadzadeh; a.mzadeh@ieee.org and Saleh Mobayen; mobayens@yuntech.edu.tw

Received 5 January 2022; Revised 23 February 2022; Accepted 23 April 2022; Published 20 June 2022

Academic Editor: Hiroki Sayama

In this paper, a new approach is presented for stabilizing and synchronizing financial chaotic systems. A new type-3 (T3) fuzzy-based system (FLS) with an online optimization scheme is designed to cope with chaotic behavior, high-level uncertainties, and unknown dynamics. An adaptive compensator also eliminates the effect of approximation errors (AEs) and perturbations. The stability of the dynamics of synchronization errors is guaranteed by the use of the Lyapunov method. Several simulations and comparisons demonstrate the superiority of the suggested control and synchronization scenarios.

1. Introduction

Chaos theory studies the mathematical formulation and behavior of dynamic systems sensitive to initial conditions. Chaos often has been seen as an interdisciplinary theory for exploring the randomness of complex chaotic systems to identify fundamental fractals, self-organization, basic patterns, fixed feedback loops, repetitions, and self-similarities. These special features have provided good potential applications for chaotic systems. Recently, various applications have been reported for chaotic systems such as image encryption [1], chaotic maps [2], time series [3], optimization algorithms [4], medical systems [5], and secure communications [6].

The control of chaotic systems (CSs) is a complex control problem because of their complex nonlinear dynamics, high senility to the initial condition, hard dynamic perturbation in most of their applications, and stochastic dynamical behavior such as symmetry and dissipation. The controllers in this field can be classified into three classes: classical methods, neuro-fuzzy controllers, and hybrid control methods.

For the first class, some model-based controllers have been presented. For example, in [7], the passivity-based approach is developed using a sliding-mode controller (SMC) and it is applied for unified CSs. In [8], bifurcation analyses are presented for a CS, and by the Lyapunov method, a robust synchronization scheme is proposed. The feedback controller is designed in [9], and the stability is investigated using the Barbashin–Krasovskii approach. The adaptive SMC is studied in [10], and its accuracy is evaluated on chameleon CSs. In [11], the behavior of CSs is analyzed

and by the use of the finite-time stability theorem, the stability is studied in various conditions. In [12], the SMC scheme is developed and the bifurcation diagrams are analyzed. In [13], a fixed-time convergence scheme is presented for memductance-based CSs and the robustness is examined under bounded perturbations. In [14], the bifurcation of butterflyfish CSs is investigated and a linear control method is suggested for synchronization. The model-based adaptive controller is developed in [15] to investigate the stability of a generator of nuclear spin CSs. The projective control systems and synchronization of CSs are studied in [16].

The FLSs and neural networks (NNs) are widely used to cope with uncertainties. For chaotic systems, some neuro-fuzzy methods have also been studied. For example, in [17], NNs are used for prediction problems in Hyperjerk CSs and their physical circuit implementation is investigated. The finite-time synchronization of CSs is studied in [18] and, by analyzing the convergence time, an FLS-based controller is presented. In [19], the synchronization problem is studied by the use of NNs and the designed synchronized scheme is applied for a secure communication system. In [20], a Takagi–Sugeno FLS is used for modeling and a sampled-data control system is developed for synchronization. The FLS-based SMC is formulated in [21], and the better performance of FLS-based schemes is shown by applying a gyroscope CS. The backstepping SMC is suggested in [22] for stabilizing CSs in the presence of time delay, and FLSs are used to estimate some nonlinearities. In [23], based on reinforcement learning and FLSs, a synchronization scheme is developed. The performance of FLS-based synchronization methods is evaluated and analyzed in [24]. In [25], improvement of the synchronization accuracy and the convergence speed is studied by the use of FLSs. In [26, 27], the superiority of FLS-based controllers in robotic applications is studied.

The financial CSs are widely used in economic problems [28–30]. The dynamics of these classes of chaotic systems are much more complex because of the existence of various unpredictable factors. The stabilization and synchronization of financial CSs have been rarely studied. For example, the integral SMC is designed in [31] and the stabilizing conditions are studied. Similarly, the terminal SMC is developed in [32] and the control of a financial CS is analyzed. In [33], an H_∞-based control system is designed and FLSs are used to investigate the robustness. The risk assessment of financial CSs is investigated in [34], and an FLS-based method is presented. In [35], an FLS-based system is proposed for forecasting applications. The finite-time control of hypercritic financial systems is investigated in [36], and some adaptation rules are suggested for stabilizing. A neuro-fuzzy-based controller is designed in [37] to guarantee the stability of the financial CS.

The literature reviewing show that

(i) In most studies, the controller is designed for a special case of CS and the designed controller cannot be applied for a CS with different parameters and dynamics [7–9]

(ii) The stability of most reviewed controllers is not guaranteed under perturbations and uncertainties [30, 38]

(iii) Some type-1 and type-2 neuro-fuzzy controllers have been developed for CSs, but most of them cannot handle the high uncertainties in CS dynamics [33–37]

(iv) Most of the previous studies are optimized in an offline scheme [33–37]

(v) The robustness against unknown perturbations in CS dynamics needs more studies [9, 36, 37]

Regarding the above discussion, a new type-3 fuzzy-based controller is developed for CSs. Most recently, the type-3 FLSs with strong uncertainty modeling capability have been developed. In various studies, it has been shown that the T3-FLSs result in much better performance in a high-noisy environment [39]. Some T3-FLS-based controllers have been developed MEMS gyroscopes and a class of fractional-order CSs [39–41]. In these studies, the T3-FLS-based controllers are developed for first-order fractional-order CSs and the special cases of MEMS gyroscopes. To the best of our knowledge, stable and robust controllers based on T3-FLSs have not been studied for financial CSs. As mentioned earlier, this class of CSs exhibits a complex stochastic behavior and their dynamics is perturbed in most applications. In this study, a new control scenario is suggested on basis of T3-FLSs. The designed T3-FLSs are optimized by the Lyapunov learning rules. The robustness is analyzed in both stabilization and synchronization problems, and an adaptive compensator is developed to deal with AEs. The main contributions are

(i) The designed controller does not depend on the parameters and dynamics of the case study CS. It can be easily applied for the various cases of CSs.

(ii) The stability is ensured under perturbations and uncertainties.

(iii) A T3-FLS-based approach is developed for better handling the uncertainties.

(iv) The suggested controller is tuned in an online scheme. In other words, the free parameters of the T3-FLS are tuned at each sample time. This approach can handle unpredicted perturbations.

(v) The robustness is studied, and a compensator is developed.

2. Problem Formulation

The following financial CSs are considered [42]:

$$\begin{aligned}\dot{\chi}_1 &= (-a + \chi_2)\chi_1 + \chi_3,\\ \dot{\chi}_2 &= -b\chi_2 - \chi_1^2 + 1,\\ \dot{\chi}_3 &= -\chi_1 - c\chi_3,\end{aligned} \tag{1}$$

where b denotes the investment cost, a represents the saving amount, c is elasticity of commercial demands, $\dot{\chi}_1$ is the interest rate, $\dot{\chi}_2$ represents investment demand, and $\dot{\chi}_3$ is the price exponent. The bifurcation and the Lyapunov spectrum analysis have been studied in [43, 44]. The phase portraits are depicted in Figure 1 that shows the chaotic attractors.

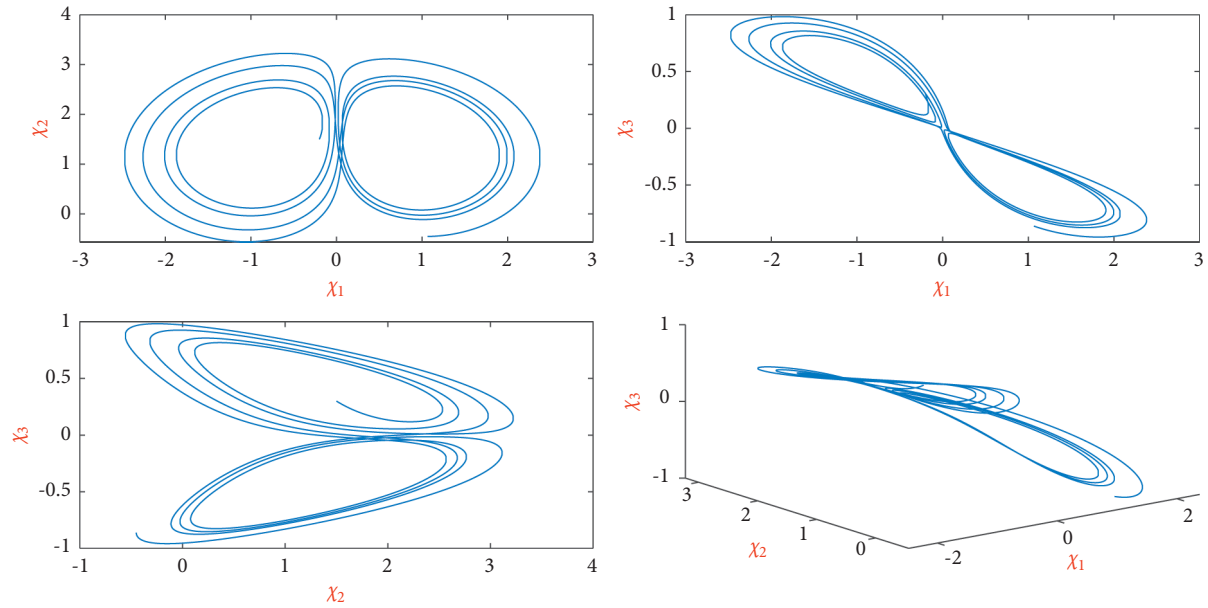

Figure 1: Phase portrait.

The variation of the investment cost, the saving amount, and elasticity of commercial demands are assumed to be unknown, and also the dynamics is unknown. The suggested T3-FLS is used to cope with variations of parameters and dynamic uncertainties and perturbations. The suggested control diagram is shown in Figure 2. We see that T3-FLSs are optimized such that all states are stabilized and the outputs track the reader system. The compensators deal with the perturbations.

Remark 1. The case study CS 1 is considered in this paper because it is so popular in the field of economic plants, and it exhibits more complex chaotic behavior. However, the suggested controller does not depend on the dynamics, and it can be easily applied for the various cases of CSs.

3. Type-3 FLS

The neuro-fuzzy systems and learning methods are extensively used to tackle uncertainties. In this paper, a new stronger approach is formulated to cope with uncertainties in the complex dynamics of CSs. The suggested FLS scheme is depicted in Figure 3. All uncertainties are tackled using optimized T3-FLSs. The computations are given as follows:

(1) The inputs of the T3-FLS ψ_i are χ_1, χ_2, and χ_3.

(2) For inputs χ_1, χ_2, and χ_3, the Gaussian MFs as shown in Figure 4 are considered. Unlike the type-2 MFs, in type-3 MFs, we have four membership values for each horizontal slice. Two of them are associated with the lower cut and the other two for the upper cut. The MFs for χ_i are defined as Ω and $\bar{\Omega}_i$ (see Figure 4). The centers of Ω and $\bar{\Omega}_i^j$ are determined considering the upper/lower bounds $\bar{\Omega}_i$. For χ_i, the upper memberships of $\bar{\Omega}_{\chi_i}$ and $\underline{\Omega}_{\chi_i}$, considering the upper/lower slice $\bar{\nu}_l$/ $\underline{\nu}_l$ are written as

$$\begin{aligned}
\bar{\mu}_{\underline{\Omega}_{i,\bar{\nu}_l}}(\chi_i) &= \exp\left(-\frac{\left(\chi_i - C_{\underline{\Omega}_i}\right)^2}{\bar{\sigma}^2_{\underline{\Omega}_{i,\bar{\nu}_l}}}\right),\\
\bar{\mu}_{\underline{\Omega}_{i,\underline{\nu}_l}}(\chi_i) &= \exp\left(-\frac{\left(\chi_i - C_{\underline{\Omega}_i}\right)^2}{\bar{\sigma}^2_{\underline{\Omega}_{i,\underline{\nu}_l}}}\right),\\
\bar{\mu}_{\bar{\Omega}_{i,\bar{\nu}_l}}(\chi_i) &= \exp\left(-\frac{\left(\chi_i - C_{\bar{\Omega}_i}\right)^2}{\bar{\sigma}^2_{\bar{\Omega}_{i,\bar{\nu}_l}}}\right),\\
\bar{\mu}_{\bar{\Omega}_{i,\underline{\nu}_l}}(\chi_i) &= \exp\left(-\frac{\left(\chi_i - C_{\bar{\Omega}_i}\right)^2}{\bar{\sigma}^2_{\bar{\Omega}_{i,\underline{\nu}_l}}}\right).
\end{aligned} \tag{2}$$

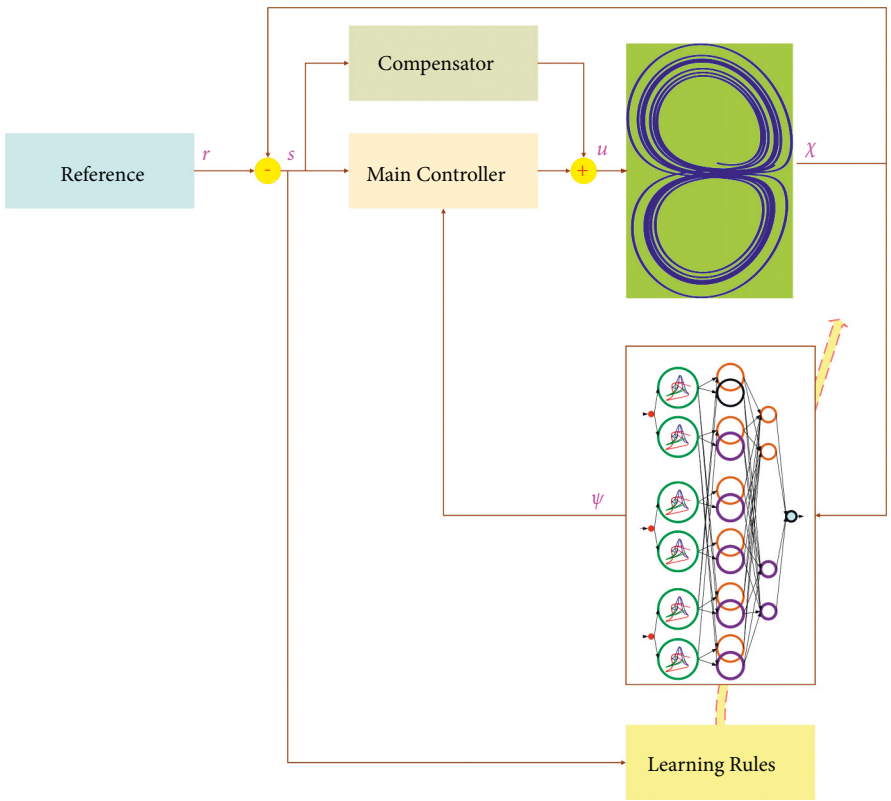

Figure 2: Control scheme.

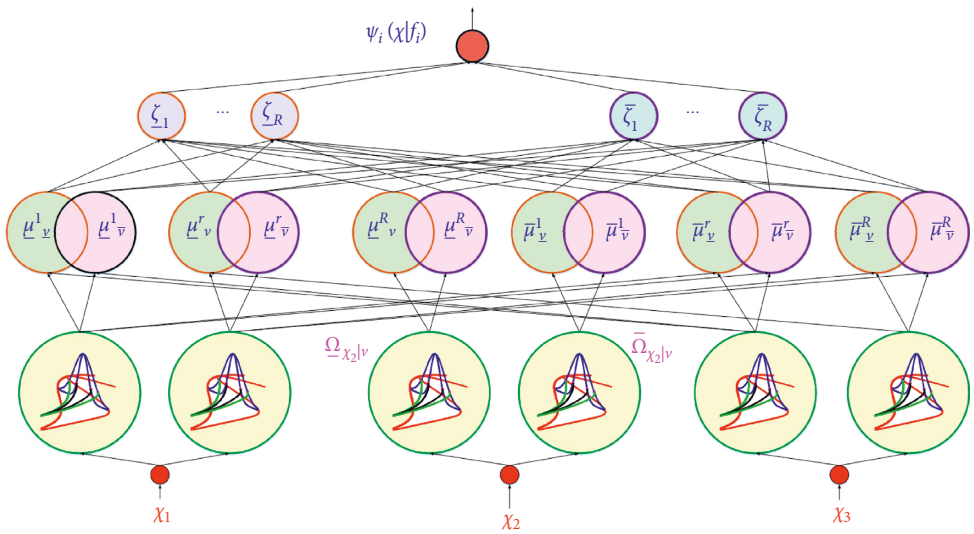

Figure 3: A schematic view of the T3-FLS.

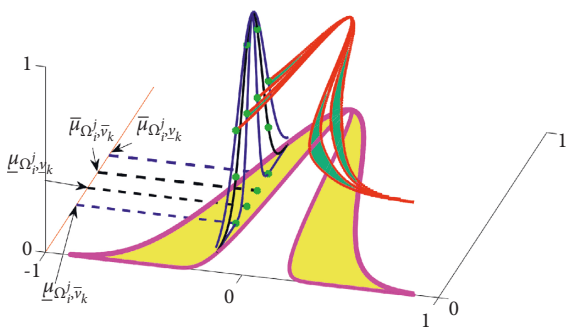

Figure 4: A schematic view of the type-3MF.

Similarly, for $\underline{\Omega}_i$, we have

$$\begin{aligned}
\mu_{\underline{\Omega}_{i,\bar{\nu}_l}}(\chi_i) &= \exp\left(-\frac{\left(\chi_i - C_{\underline{\Omega}_i}\right)^2}{\sigma^2_{\underline{\Omega}_{i,\bar{\nu}_l}}}\right),\\
\mu_{\underline{\Omega}_{i,\underline{\nu}_l}}(\chi_i) &= \exp\left(-\frac{\left(\chi_i - C_{\underline{\Omega}_i}\right)^2}{\sigma^2_{\underline{\Omega}_{i,\underline{\nu}_l}}}\right),\\
\mu_{\underline{\bar{\Omega}}_{i,\bar{\nu}_l}}(\chi_i) &= \exp\left(-\frac{\left(\chi_i - C_{\bar{\Omega}_i}\right)^2}{\sigma^2_{\bar{\Omega}_{i,\bar{\nu}_l}}}\right),\\
\mu_{\underline{\bar{\Omega}}_{i,\underline{\nu}_l}}(\chi_i) &= \exp\left(-\frac{\left(\chi_i - C_{\bar{\Omega}_i}\right)^2}{\sigma^2_{\bar{\Omega}_{i,\underline{\nu}_l}}}\right),
\end{aligned} \tag{3}$$

where $C_{\underline{\Omega}_i}$ and $C_{\bar{\Omega}_i}$ denote centers of $\underline{\Omega}_{\chi_i}$ and $\bar{\Omega}_{\chi_i}$, respectively. $\bar{\sigma}_{\underline{\Omega}_{i,\underline{\nu}_l}}$ and $\bar{\sigma}^2_{\underline{\Omega}_{i,\bar{\nu}_l}}$ represent the upper width of $\underline{\Omega}_{\chi_i}$ at the upper slice $\bar{\nu}_l$ and lower slice $\underline{\nu}_l$.

(3) In the next step, considering the memberships in step 2, the rule firings should be computed. We have R rules. The $r-th$ rule is written as

$$\begin{aligned}
&\text{Rule \#}r\text{: If } \chi_1 \text{ is } \Omega_{\chi_1,\nu_j} \text{ and } \chi_2 \text{ is } \Omega_{\chi_2,\nu_j}\\
&\text{and } \chi_3 \text{ is } \Omega_{\chi_3,\nu_j} \text{ Then } \psi \in \left[\underline{x}_r, \bar{x}_r\right],
\end{aligned} \tag{4}$$

where $\underline{x}_r, \bar{x}_r$ denote the rule parameters.

(4) By the use of the product T-norm and the simple type-reduction of [45], the output of ψ_i is written as

where $\underline{f}_i$ and ς_i are

$$\begin{aligned}
f_i &= \left[\underline{x}_{i1}, \ldots, \underline{x}_{iR}, \bar{x}_{i1}, \ldots, \bar{x}_{iR}\right]^T,\\
\varsigma_i &= \left[\underline{\varsigma}_{i1}, \ldots, \underline{\varsigma}_{iR}, \bar{\varsigma}_{i1}, \ldots, \bar{\varsigma}_{iR}\right]^T,
\end{aligned} \tag{6}$$

where R is number of rules and $\bar{x}_{ir}$ and $\underline{x}_{ir}$ represent the $r-th$ rule parameters. $\underline{\varsigma}_{ir}$ and $\bar{\varsigma}_{il}$ are

$$\begin{aligned}
\bar{\varsigma}_r &= \frac{\sum_{j=1}^{n_\nu}\left(\bar{\nu}_j\bar{\theta}^r_{\bar{\nu}_j}/\sum_{r=1}^{R}\left(\bar{\theta}^r_{\bar{\nu}_j}+\theta^r_{\underline{\nu}_j}\right)\right)}{\sum_{j=1}^{n_\nu}\left(\bar{\nu}_j+\underline{\nu}_j\right)}\\
&\quad+\frac{\sum_{j=1}^{n_\nu}\left(\underline{\nu}_j\bar{\theta}^r_{\underline{\nu}_j}/\sum_{r=1}^{R}\left(\bar{\theta}^r_{\underline{\nu}_j}+\theta^r_{\underline{\nu}_j}\right)\right)}{\sum_{j=1}^{n_\nu}\left(\bar{\nu}_j+\underline{\nu}_j\right)},\ r=1,\ldots,R,\\
\underline{\varsigma}_r &= \frac{\sum_{j=1}^{n_\nu}\left(\bar{\nu}_j\theta^r_{\bar{\nu}_j}/\sum_{r=1}^{R}\left(\bar{\theta}^r_{\bar{\nu}_j}+\theta^r_{\bar{\nu}_j}\right)\right)}{\sum_{j=1}^{n_\nu}\left(\bar{\nu}_j+\underline{\nu}_j\right)}\\
&\quad+\frac{\sum_{j=1}^{n_\nu}\left(\underline{\nu}_j\theta^r_{\underline{\nu}_j}/\sum_{r=1}^{R}\left(\bar{\theta}^r_{\underline{\nu}_j}+\theta^r_{\underline{\nu}_j}\right)\right)}{\sum_{j=1}^{n_\nu}\left(\bar{\nu}_j+\underline{\nu}_j\right)},\ r=1,\ldots,R,
\end{aligned} \tag{7}$$

where n_ν denotes slice numbers and

$$\begin{aligned}
\underline{\varsigma}_r &= \frac{\sum_{j=1}^{n_\nu}\bar{\nu}_j\theta^r_{\bar{\nu}_j}/\sum_{r=1}^{R}\left(\bar{\theta}^r_{\bar{\nu}_j}+\theta^r_{\bar{\nu}_j}\right)}{\sum_{j=1}^{n_\nu}\left(\bar{\nu}_j+\underline{\nu}_j\right)}\\
&\quad+\frac{\sum_{j=1}^{n_\nu}\underline{\nu}_j\theta^r_{\underline{\nu}_j}/\sum_{r=1}^{R}\left(\bar{\theta}^r_{\underline{\nu}_j}+\theta^r_{\underline{\nu}_j}\right)}{\sum_{j=1}^{n_\nu}\left(\bar{\nu}_j+\underline{\nu}_j\right)},\ r=1,\ldots,R,
\end{aligned} \tag{8}$$

$$\begin{aligned}
\theta^r_{\bar{\nu}_j} &= \mu_{\underline{\Omega}_{\chi_1}|\bar{\nu}_j}(\chi_1)\mu_{\underline{\Omega}_{\chi_2}|\bar{\nu}_j}(\chi_2)\mu_{\underline{\Omega}_{\chi_3}|\bar{\nu}_j}(\chi_3),\\
\theta^r_{\underline{\nu}_j} &= \mu_{\underline{\Omega}_{\chi_1}|\underline{\nu}_j}(\chi_1)\mu_{\underline{\Omega}_{\chi_2}|\underline{\nu}_j}(\chi_2)\mu_{\underline{\Omega}_{\chi_3}|\underline{\nu}_j}(\chi_3),\\
\bar{\theta}^r_{\bar{\nu}_j} &= \bar{\mu}_{\Omega_{\chi_1}|\bar{\nu}_j}(\chi_1)\bar{\mu}_{\Omega_{\chi_2}|\bar{\nu}_j}(\chi_2)\bar{\mu}_{\Omega_{\chi_3}|\bar{\nu}_j}(\chi_3),\\
\bar{\theta}^r_{\underline{\nu}_j} &= \bar{\mu}_{\Omega_{\chi_1}|\underline{\nu}_j}(\chi_1)\bar{\mu}_{\Omega_{\chi_2}|\underline{\nu}_j}(\chi_2)\bar{\mu}_{\Omega_{\chi_3}|\underline{\nu}_j}(\chi_3).
\end{aligned}$$

$$\psi_i = f_i^T\varsigma_i, \tag{5}$$

4. Stabilization

In this section, the stabilizing controller is designed and its stability conditions are analyzed. The main results are presented in Theorem 1.

Theorem 1. *The system (1) is stabilized by using controllers (17), adaptation rules (18), and compensators (19).*

$$\begin{aligned} u_i &= -\psi_i(\chi|f_i) - k_i\chi_i - u_{ci}, \\ \dot{f}_i &= \iota\varsigma_i\chi_i, \\ u_{ci} &= E_i\mathrm{sign}(\chi_i), \end{aligned} \tag{9}$$

where ι and k are constants, ψ_i denotes the T3-FLS, χ and f are the input vector and the rule parameter vector of ψ_i, respectively, and E_i is the upper bound of AE.

Proof. By applying the controllers u_i, $i = 1, 2, 3$ (17) into (1), we have

$$\begin{aligned} \dot{\chi}_1 &= (-a + \chi_2)\chi_1 + \chi_3 \\ &\quad - k_1\chi_1 - \psi_1(\chi|f_1) - u_{c1}, \\ \dot{\chi}_2 &= -b\chi_2 - \chi_1^2 + 1 \\ &\quad - k_2\chi_2 - \psi_2(\chi|f_2) - u_{c2}, \\ \dot{\chi}_3 &= -\chi_1 - c\chi_3 \\ &\quad - k_3\chi_3 - \psi_3(\chi|f_3) - u_{c3}. \end{aligned} \tag{10}$$

From (31), $\dot{\chi}$ is written as

$$\begin{aligned} \dot{\chi}_1 &= (-a + \chi_2)\chi_1 + \chi_3 \\ &\quad - k_1\chi_1 - \psi_1(\chi|f_1) - u_{c1}, \\ \dot{\chi}_2 &= -b\chi_2 - \chi_1^2 + 1 \\ &\quad - k_2\chi_2 - \psi_2(\chi|f_2) - u_{c2}, \\ \dot{\chi}_3 &= -\chi_1 - c\chi_3 \\ &\quad - k_3\chi_3 - \psi_3(\chi|f_3) - u_{c3}. \end{aligned} \tag{11}$$

The optimal T3-FLSs ($\psi_i^*(\chi|f_i^*)$) are defined as T3-FLSs with optimal parameters (f_i^*). The optimal T3-FLSs are added and subtracted into (32); then, we have

$$\begin{aligned} \dot{\chi}_1 &= (-a + \chi_2)\chi_1 + \chi_3 \\ &\quad - k_1\chi_1 - \psi_1(\chi|f_1) - u_{c1} \\ &\quad + \psi_1^*(\chi|f_1^*) - \psi_1^*(\chi|f_1^*), \\ \dot{\chi}_2 &= -b\chi_2 - \chi_1^2 + 1 \\ &\quad - k_2\chi_2 - \psi_2(\chi|f_2) - u_{c2} \\ &\quad + \psi_2^*(\chi|f_2^*) - \psi_2^*(\chi|f_2^*), \\ \dot{\chi}_3 &= -\chi_1 - c\chi_3 \\ &\quad - k_3\chi_3 - \psi_3(\chi|f_3) - u_{c3} \\ &\quad + \psi_3^*(\chi|f_3^*) - \psi_3^*(\chi|f_3^*). \end{aligned} \tag{12}$$

By simplification, the dynamics of χ_i, $i = 1, 2, 3$ in (33) is rewritten as

$$\begin{aligned} \dot{\chi}_1 &= \psi_1^*(\chi|f_1^*) - \psi_1(\chi|f_1) \\ &\quad - k_1\chi_1 - u_{c1} \\ &\quad + (-a + \chi_2)\chi_1 + \chi_3 - \psi_1^*(\chi|f_1^*), \end{aligned} \tag{13}$$

$$\begin{aligned} \dot{\chi}_2 &= \psi_2^*(\chi|f_2^*) - \psi_2(\chi|f_2) \\ &\quad - k_2\chi_2 - u_{c2} \\ &\quad - b\chi_2 - \chi_1^2 + 1 - \psi_2^*(\chi|f_2^*), \end{aligned} \tag{14}$$

$$\begin{aligned} \dot{\chi}_3 &= \psi_3^*(\chi|f_3^*) - \psi_3(\chi|f_3) \\ &\quad - k_3\chi_3 - u_{c3} \\ &\quad - \chi_1 - c\chi_3 - \psi_3^*(\chi|f_3^*). \end{aligned} \tag{15}$$

By the use of the vector from (5) we have

$$\begin{aligned} \dot{\chi}_1 &= \tilde{f}_1^T\varsigma_1 \\ &\quad - k_1\chi_1 - u_{c1} \\ &\quad + (-a + \chi_2)\chi_1 + \chi_3 - \psi_1^*(\chi|f_1^*), \\ \dot{\chi}_2 &= \tilde{f}_2^T\varsigma_2 \\ &\quad -k_2\chi_2 - u_{c2} \\ &\quad -b\chi_2 - \chi_1^2 + 1 - \psi_2^*(\chi|f_2^*), \\ \dot{\chi}_3 &= \tilde{f}_3^T\varsigma_3 \\ &\quad -k_3\chi_3 - u_{c3} \\ &\quad -\chi_1 - c\chi_3 - \psi_3^*(\chi|f_3^*), \end{aligned} \tag{16}$$

where $\tilde{f}_i = f_i^* - f_i$. For stability investigation, to prove the results of Theorem 1, a Lyapunov candidate is considered as

$$\begin{aligned} V &= \frac{1}{2\iota}\chi_1^2 + \frac{1}{2\iota}\chi_2^2 + \frac{1}{2\iota}\chi_3^2 \\ &\quad + \frac{1}{2\iota}\tilde{f}_1^T\tilde{f}_1 + \frac{1}{2\iota}\tilde{f}_2^T\tilde{f}_2 + \frac{1}{2\iota}\tilde{f}_3^T\tilde{f}_3. \end{aligned} \tag{17}$$

The time derivative of (38) yields

$$\begin{aligned} \dot{V} &= \frac{1}{\iota}\dot{\chi}_1\chi_1 + \frac{1}{\iota}\dot{\chi}_2\chi_2 + \frac{1}{\iota}\dot{\chi}_3\chi_3 \\ &\quad -\frac{1}{\iota}\tilde{f}_1^T\dot{f}_1 - \frac{1}{\iota}\tilde{f}_2^T\dot{f}_2 - \frac{1}{\iota}\tilde{f}_3^T\dot{f}_3. \end{aligned} \tag{18}$$

Substituting from $\dot{\chi}_i$, $i = 1, 2, 3$ (26)–(28) into (39), we obtain

$$\begin{aligned}\dot{V} = &\begin{bmatrix} \tilde{f}_1^T \varsigma_1 - k_1\chi_1 - u_{c1} \\ +(-a+\chi_2)\chi_1 + \chi_3 - \psi_1^*(\chi|f_1^*) \end{bmatrix}\chi_1 \\ &+ \begin{bmatrix} \tilde{f}_2^T \varsigma_2 - k_2\chi_2 - u_{c2} \\ -b\chi_2 - \chi_1^2 + 1 - \psi_2^*(\chi|f_2^*) \end{bmatrix}\chi_2 \\ &+ \begin{bmatrix} \tilde{f}_3^T \varsigma_3 - k_3\chi_3 - u_{c3} \\ -\chi_1 - c\chi_3 - \psi_3^*(\chi|f_3^*) \end{bmatrix}\chi_3 \\ &- \frac{1}{\iota}\tilde{f}_1^T \dot{f}_1 - \frac{1}{\iota}\tilde{f}_2^T \dot{f}_2 - \frac{1}{\iota}\tilde{f}_3^T \dot{f}_3. \end{aligned} \tag{19}$$

Equation (40) can be rewritten as

$$\begin{aligned}\dot{V} = &-k_1\chi_1^2 + \tilde{f}_1^T \varsigma_1\chi_1 - \frac{1}{\iota}\tilde{f}_1^T \dot{f}_1 - u_{c1}\chi_1 \\ &- k_2\chi_2^2 + \tilde{f}_2^T \varsigma_2\chi_2 - \frac{1}{\iota}\tilde{f}_2^T \dot{f}_2 - u_{c2}\chi_2 \\ &- k_3\chi_3^2 + \tilde{f}_3^T \varsigma_3\chi_3 - \frac{1}{\iota}\tilde{f}_3^T \dot{f}_3 - u_{c3}\chi_3 \\ &+ [(-a+\chi_2)\chi_1 + \chi_3 - \psi_1^*(\chi|f_1^*)]\chi_1 \\ &+ \left[-b\chi_2 - \chi_1^2 + 1 - \psi_2^*(\chi|f_2^*)\right]\chi_2 \\ &+ [-\chi_1 - c\chi_3 - \psi_3^*(\chi|f_3^*)]\chi_3. \end{aligned} \tag{20}$$

Equation (11) is simplified as

$$\begin{aligned}\dot{V} = &-k_1\chi_1^2 + \tilde{f}_1^T\left(\varsigma_1\chi_1 - \frac{1}{\iota}\dot{f}_1\right) - u_{c1}\chi_1 \\ &- k_2\chi_2^2 + \tilde{f}_2^T\left(\varsigma_2\chi_2 - \frac{1}{\iota}\dot{f}_2\right) - u_{c2}\chi_2 \\ &- k_3\chi_3^2 + \tilde{f}_3^T\left(\varsigma_3\chi_3 - \frac{1}{\iota}\dot{f}_3\right) - u_{c3}\chi_3 \\ &+ [(-a+\chi_2)\chi_1 + \chi_3 - \psi_1^*(\chi|f_1^*)]\chi_1 \\ &+ \left[-b\chi_2 - \chi_1^2 + 1 - \psi_2^*(\chi|f_2^*)\right]\chi_2 \\ &+ [-\chi_1 - c\chi_3 - \psi_3^*(\chi|f_3^*)]\chi_3. \end{aligned} \tag{21}$$

Considering the tuning rules (18), from (42), we obtain

$$\begin{aligned}\dot{V} = &-k_1\chi_1^2 - k_2\chi_2^2 - k_3\chi_3^2 \\ &- u_{c1}\chi_1 - u_{c2}\chi_2 - u_{c3}\chi_3 \\ &+ [(-a+\chi_2)\chi_1 + \chi_3 - \psi_1^*(\chi|f_1^*)]\chi_1 \\ &+ \left[-b\chi_2 - \chi_1^2 + 1 - \psi_2^*(\chi|f_2^*)\right]\chi_2 \\ &+ [-\chi_1 - c\chi_3 - \psi_3^*(\chi|f_3^*)]\chi_3. \end{aligned} \tag{22}$$

From (43), we have

$$\begin{aligned}\dot{V} \le &-k_1\chi_1^2 - k_2\chi_2^2 - k_3\chi_3^2 \\ &- u_{c1}\chi_1 - u_{c2}\chi_2 - u_{c3}\chi_3 \\ &+ \left|(-a+\chi_2)\chi_1 + \chi_3 - \psi_1^*(\chi|f_1^*)\right||\chi_1| \\ &+ \left|-b\chi_2 - \chi_1^2 + 1 - \psi_2^*(\chi|f_2^*)\right||\chi_2| \\ &+ \left|-\chi_1 - c\chi_3 - \psi_3^*(\chi|f_3^*)\right||\chi_3|. \end{aligned} \tag{23}$$

By applying the u_{ci} from (9), we have

$$\begin{aligned}\textbf{ERROR!!}V \le &-k_1\chi_1^2 - k_2\chi_2^2 - k_3\chi_3^2 \\ &+ \left\{\left|(-a+\chi_2)\chi_1 + \chi_3 - \psi_1^*(\chi|f_1^*)\right| - E_1\right\}|\chi_1| \\ &+ \left\{\left|-b\chi_2 - \chi_1^2 + 1 - \psi_2^*(\chi|f_2^*)\right| - E_2\right\}|\chi_2| \\ &+ \left\{\left|-\chi_1 - c\chi_3 - \psi_3^*(\chi|f_3^*)\right| - E_3\right\}|\chi_3|. \end{aligned} \tag{24}$$

Considering the fact that

$$\left|(-a+\chi_2)\chi_1 + \chi_3 - \psi_1^*(\chi|f_1^*)\right| < E_1, \tag{25}$$

$$\left|-b\chi_2 - \chi_1^2 + 1 - \psi_2^*(\chi|f_2^*)\right| < E_2, \tag{26}$$

$$\left|-\chi_1 - c\chi_3 - \psi_3^*(\chi|f_3^*)\right| < E_3. \tag{27}$$

We can write $\dot{V} < 0$, and then, the proof is completed. □

5. Synchronization

In this section, the synchronization controller is designed and its stability conditions are analyzed.

Theorem 2. *System (1) tracks the leader states (r_i) by using controller (28), adaptation rules (29), and compensator (30).*

$$u_i = \dot{r}_i - \psi_i(s|f_i) - k_i s_i - u_{ci}, \tag{28}$$

$$\dot{f}_i = \iota\varsigma_i s_i, \tag{29}$$

$$u_{ci} = E_i \text{sign}(s_i), \tag{30}$$

where ι and k are constants, ψ_i denotes the T3-FLS, s_i is defined as $s_i = \chi_i - r_i$, the input vector s is defined as $s = [s_1, \ldots, s_n]^T$ and n represents the state number, f is the rule parameter vector of ψ_i, respectively, and E_i is the upper bound of AE.

Proof. By applying the controllers u_i, $i = 1, 2, 3$ (28), the dynamics of (47) is written as

$$\begin{aligned}\dot{s}_1 = &(-a+\chi_2)\chi_1 + \chi_3 \\ &- k_1 s_1 - \psi_1(s|f_1) - u_{c1}, \\ \dot{s}_2 = &-b\chi_2 - \chi_1^2 + 1 \\ &- k_2 s_2 - \psi_2(s|f_2) - u_{c2}, \\ \dot{s}_3 = &-\chi_1 - c\chi_3 \\ &- k_3 s_3 - \psi_3(s|f_3) - u_{c3}. \end{aligned} \tag{31}$$

From (31), $\dot{s}$ is written as

$$\begin{aligned}\dot{s}_1 &= (-a+\chi_2)\chi_1+\chi_3\\ &\quad -k_1s_1-\psi_1(s|f_1)-u_{c1},\\ \dot{s}_2 &= -b\chi_2-\chi_1^2+1\\ &\quad -k_2s_2-\psi_2(s|f_2)-u_{c2},\\ \dot{s}_3 &= -\chi_1-c\chi_3\\ &\quad -k_3s_3-\psi_3(s|f_3)-u_{c3}.\end{aligned} \tag{32}$$

Similar to the proof of Theorem 2, the optimal T3-FLSs are added and subtracted into (32); then, we have

$$\begin{aligned}\dot{s}_1 &= (-a+\chi_2)\chi_1+\chi_3\\ &\quad -k_1s_1-\psi_1(s|f_1)-u_{c1}\\ &\quad +\psi_1^*(s|f_1^*)-\psi_1^*(s|f_1^*),\\ \dot{s}_2 &= -b\chi_2-\chi_1^2+1\\ &\quad -k_2s_2-\psi_2(s|f_2)-u_{c2}\\ &\quad +\psi_2^*(s|f_2^*)-\psi_2^*(s|f_2^*),\\ \dot{s}_3 &= -\chi_1-c\chi_3\\ &\quad -k_3s_3-\psi_3(s|f_3)-u_{c3}\\ &\quad +\psi_3^*(s|f_3^*)-\psi_3^*(s|f_3^*).\end{aligned} \tag{33}$$

The dynamics of (33) is rewritten as

$$\begin{aligned}\dot{s}_1 &= \psi_1^*(s|f_1^*)-\psi_1(s|f_1)\\ &\quad -k_1s_1-u_{c1}\\ &\quad +(-a+\chi_2)\chi_1+\chi_3-\psi_1^*(s|f_1^*),\\ \dot{s}_2 &= \psi_2^*(s|f_2^*)-\psi_2(s|f_2)\\ &\quad -k_2s_2-u_{c2}\\ &\quad -b\chi_2-\chi_1^2+1-\psi_2^*(s|f_2^*),\\ \dot{s}_3 &= \psi_3^*(s|f_3^*)-\psi_3(s|f_3)\\ &\quad -k_3s_3-u_{c3}\\ &\quad -\chi_1-c\chi_3-\psi_3^*(s|f_3^*).\end{aligned} \tag{34}$$

By the use of the vector form (5), we have

$$\begin{aligned}\dot{s}_1 &= \tilde{f}_1^T\varsigma_1\\ &\quad -k_1s_1-u_{c1}\\ &\quad +(-a+\chi_2)\chi_1+\chi_3-\psi_1^*(s|f_1^*),\end{aligned} \tag{35}$$

$$\dot{s}_2=\tilde{f}_2^T\varsigma_2-k_2s_2-u_{c2}-b\chi_2-\chi_1^2+1-\psi_2^*(s|f_2^*), \tag{36}$$

$$\dot{s}_3=\tilde{f}_3^T\varsigma_3-k_3s_3-u_{c3}-\chi_1-c\chi_3-\psi_3^*(s|f_3^*), \tag{37}$$

where $\tilde{f}_i=f_i^*-f_i$. To prove the results of Theorem 2, a Lyapunov candidate is considered as

$$\begin{aligned}V &= \frac{1}{2\iota}s_1^2+\frac{1}{2\iota}s_2^2+\frac{1}{2\iota}s_3^2\\ &\quad +\frac{1}{2\iota}\tilde{f}_1^T\tilde{f}_1+\frac{1}{2\iota}\tilde{f}_2^T\tilde{f}_2+\frac{1}{2\iota}\tilde{f}_3^T\tilde{f}_3.\end{aligned} \tag{38}$$

The time derivative of (38) yields

$$\begin{aligned}\dot{V} &= \frac{1}{\iota}\dot{s}_1s_1+\frac{1}{\iota}\dot{s}_2s_2+\frac{1}{\iota}\dot{s}_3s_3\\ &\quad -\frac{1}{\iota}\tilde{f}_1^T\dot{f}_1-\frac{1}{\iota}\tilde{f}_2^T\dot{f}_2-\frac{1}{\iota}\tilde{f}_3^T\dot{f}_3.\end{aligned} \tag{39}$$

Substituting $\dot{s}_i$, $i=1,2,3$, from (35)–(37), we obtain

$$\begin{aligned}\dot{V} &= \begin{bmatrix}\tilde{f}_1^T\varsigma_1-k_1s_1-u_{c1}\\ +(-a+\chi_2)\chi_1+\chi_3-\psi_1^*(s|f_1^*)\end{bmatrix}s_1\\ &\quad +\begin{bmatrix}\tilde{f}_2^T\varsigma_2-k_2s_2-u_{c2}\\ -b\chi_2-\chi_1^2+1-\psi_2^*(s|f_2^*)\end{bmatrix}s_2\\ &\quad +\begin{bmatrix}\tilde{f}_3^T\varsigma_3-k_3s_3-u_{c3}\\ -\chi_1-c\chi_3-\psi_3^*(s|f_3^*)\end{bmatrix}s_3\\ &\quad -\frac{1}{\iota}\tilde{f}_1^T\dot{f}_1-\frac{1}{\iota}\tilde{f}_2^T\dot{f}_2-\frac{1}{\iota}\tilde{f}_3^T\dot{f}_3.\end{aligned} \tag{40}$$

Equation (40) can be rewritten as

$$\begin{aligned}\dot{V} &= -k_1s_1^2+\tilde{f}_1^T\varsigma_1s_1-\frac{1}{\iota}\tilde{f}_1^T\dot{f}_1-u_{c1}s_1\\ &\quad -k_2s_2^2+\tilde{f}_2^T\varsigma_2s_2-\frac{1}{\iota}\tilde{f}_2^T\dot{f}_2-u_{c2}s_2\\ &\quad -k_3s_3^2+\tilde{f}_3^T\varsigma_3s_3-\frac{1}{\iota}\tilde{f}_3^T\dot{f}_3-u_{c3}s_3\\ &\quad +[(-a+\chi_2)\chi_1+\chi_3-\psi_1^*(s|f_1^*)]s_1\\ &\quad +\left[-b\chi_2-\chi_1^2+1-\psi_2^*(s|f_2^*)\right]s_2\\ &\quad +[-\chi_1-c\chi_3-\psi_3^*(s|f_3^*)]s_3.\end{aligned} \tag{41}$$

Equation (29) is simplified as

$$\begin{aligned}\dot{V} &= -k_1s_1^2+\tilde{f}_1^T\left(\varsigma_1\chi_1-\frac{1}{\iota}\dot{f}_1\right)-u_{c1}s_1\\ &\quad -k_2s_2^2+\tilde{f}_2^T\left(\varsigma_2\chi_2-\frac{1}{\iota}\dot{f}_2\right)-u_{c2}s_2\\ &\quad -k_3s_3^2+\tilde{f}_3^T\left(\varsigma_3\chi_3-\frac{1}{\iota}\dot{f}_3\right)-u_{c3}s_3\\ &\quad +[(-a+\chi_2)\chi_1+\chi_3-\psi_1^*(s|f_1^*)]s_1\\ &\quad +\left[-b\chi_2-\chi_1^2+1-\psi_2^*(s|f_2^*)\right]s_2\\ &\quad +[-\chi_1-c\chi_3-\psi_3^*(s|f_3^*)]s_3.\end{aligned} \tag{42}$$

Considering the tuning rules (29), we obtain

$$\begin{aligned}\dot{V} = &-k_1 s_1^2 - k_2 s_2^2 - k_3 s_3^2 \\ &- u_{c1} s_1 - u_{c2} s_2 - u_{c3} s_3 \\ &+ [(-a + \chi_2)\chi_1 + \chi_3 - \psi_1^*(s|f_1^*)] s_1 \\ &+ \left[-b\chi_2 - \chi_1^2 + 1 - \psi_2^*(s|f_2^*)\right] s_2 \\ &+ [-\chi_1 - c\chi_3 - \psi_3^*(s|f_3^*)] s_3.\end{aligned} \tag{43}$$

From (43), we have

$$\begin{aligned}\dot{V} \le &-k_1 s_1^2 - k_2 s_2^2 - k_3 s_3^2 \\ &- u_{c1} s_1 - u_{c2} s_2 - u_{c3} s_3 \\ &+ \left|(-a + \chi_2)\chi_1 + \chi_3 - \psi_1^*(s|f_1^*)\right| |s_1| \\ &+ \left|-b\chi_2 - \chi_1^2 + 1 - \psi_2^*(s|f_2^*)\right| |s_2| \\ &+ \left|-\chi_1 - c\chi_3 - \psi_3^*(s|f_3^*)\right| |s_3|.\end{aligned} \tag{44}$$

By applying u_{ci} from (9), we have

$$\begin{aligned}\dot{V} \le &-k_1 s_1^2 - k_2 s_2^2 - k_3 s_3^2 \\ &+ \left\{\left|(-a + \chi_2)\chi_1 + \chi_3 - \psi_1^*(s|f_1^*)\right| - E_1\right\} |s_1| \\ &+ \left\{\left|-b\chi_2 - \chi_1^2 + 1 - \psi_2^*(s|f_2^*)\right| - E_2\right\} |s_2| \\ &+ \left\{\left|-\chi_1 - c\chi_3 - \psi_3^*(s|f_3^*)\right| - E_3\right\} |s_3|.\end{aligned} \tag{45}$$

Considering the fact that

$$\begin{aligned}\left|(-a + s_2)s_1 + s_3 - \psi_1^*(s|f_1^*)\right| < E_1, \\ \left|-bs_2 - s_1^2 + 1 - \psi_2^*(s|f_2^*)\right| < E_2, \\ \left|-s_1 - cs_3 - \psi_3^*(s|f_3^*)\right| < E_3,\end{aligned} \tag{46}$$

we can write, $\dot{V} < 0$, and then, the proof is completed. □

6. Simulation

By various simulations, the feasibility and accuracy of the stabilizing and synchronization scheme are verified.

6.1. Stabilization. In this section, the dynamics of (1) is stabilized by controller (17), tuning rules (18), and compensator (19). The simulation conditions are described in Table 1. The initial conditions are as follows: $\chi_1(0) = -0.20$, $\chi_2(0) = 1.50$, and $\chi_3(0) = 0.30$. The dynamics is unknown. A general view on the simulation scheme is depicted in Figure 5. The trajectories of outputs χ_1, χ_2, and χ_3 are depicted in Figure 6. We see that signals χ_1, χ_2, and χ_3 are well converged to zero. The corresponding control signals u_1, u_2, and u_3 are given in Figure 7, and the outputs of T3-FLSs (ψ_1, ψ_2, and ψ_3) are depicted in Figure 8. To better see the convergence to the zero point, the phase portrait is shown in Figure 9. We see that the phase trajectories have well reached the origin at a finite time.

Table 1: Simulation condition.

Parameter	Value	Equation
C_{Ω_i}	−1	(7)
$C_{\overline{\Omega}_i}$	1	(3)
$\overline{\nu}$	0.7, 0.8, and 1	(3)
$\underline{\nu}$	0.1, 0.3, and 4	(7)
k_i	100	(17)
ι	0.1	(18)
E_i	100	(19)
Algorithm type	ode3(Bogacki–Shampine)	
Integration step	0.001	
Truncation errors	0.001	

6.2. Synchronization. In this section, the synchronization accuracy is examined. The chaotic system (1) is considered as a leader system, and the slave financial chaotic system is assumed as follows:

$$\begin{aligned}\dot{r}_1 &= 0.8(r_2(t) - r_1(t)) + u_1(t), \\ \dot{r}_2 &= 0.2r_1(t) - r_2(t) - r_1(t)r_3(t) + u_2(t), \\ \dot{r}_3 &= r_1(t)r_2(t) - 1.9r_3(t) + u_3(t).\end{aligned} \tag{47}$$

System (47) is synchronized with (1) by using controller (40), tuning rules (41), and compensator (42). The simulation conditions are the same as those of the previous section. The initial conditions are as follows: $r_1(0) = -0.20$, $r_2(0) = 1.50$, $r_3(0) = 0.30$, $\chi_1(0) = 1.0$, $\chi_2(0) = -2.0$, and $\chi_3(0) = 5.0$. The trajectories of outputs χ_1, r_1, χ_2, r_2, and χ_3, r_3 are depicted in Figure 10. We see that signals χ_1, χ_2, and χ_3 are well converged to r_1, r_2, and r_3. The synchronization errors in Figure 11 show a good synchronization performance. The corresponding control signals u_1, u_2, and u_3 are given in Figure 12, and the outputs of T3-FLSs (ψ_1, ψ_2, and ψ_3) are depicted in Figure 13. To better see the synchronization, the phase portrait is shown in Figure 14. We see that the phase trajectories of the slave system have well reached the leader system at a finite time.

6.3. High Noisy Condition and Comparison. In this section, a high perturbation is applied to the system as shown in Figure 15. The simulation conditions are the same as those of the previous examination. The trajectories of outputs χ_1, r_1, χ_2, r_2, and χ_3, r_3 are depicted in Figure 16. We see that the perturbations are well tackled, and the signals χ_1, χ_2, and χ_3 are well converged to r_1, r_2, and r_3. The synchronization errors are shown in Figure 17 that shows a desired synchronization under high-level disturbances. The corresponding control signals u_1, u_2, and u_3 are given in Figure 18, and the phase portrait is shown in Figure 19. We see that similar to the previous examination, the phase trajectories of the slave system have well reached the leader system at a finite time in the presence of noisy conditions.

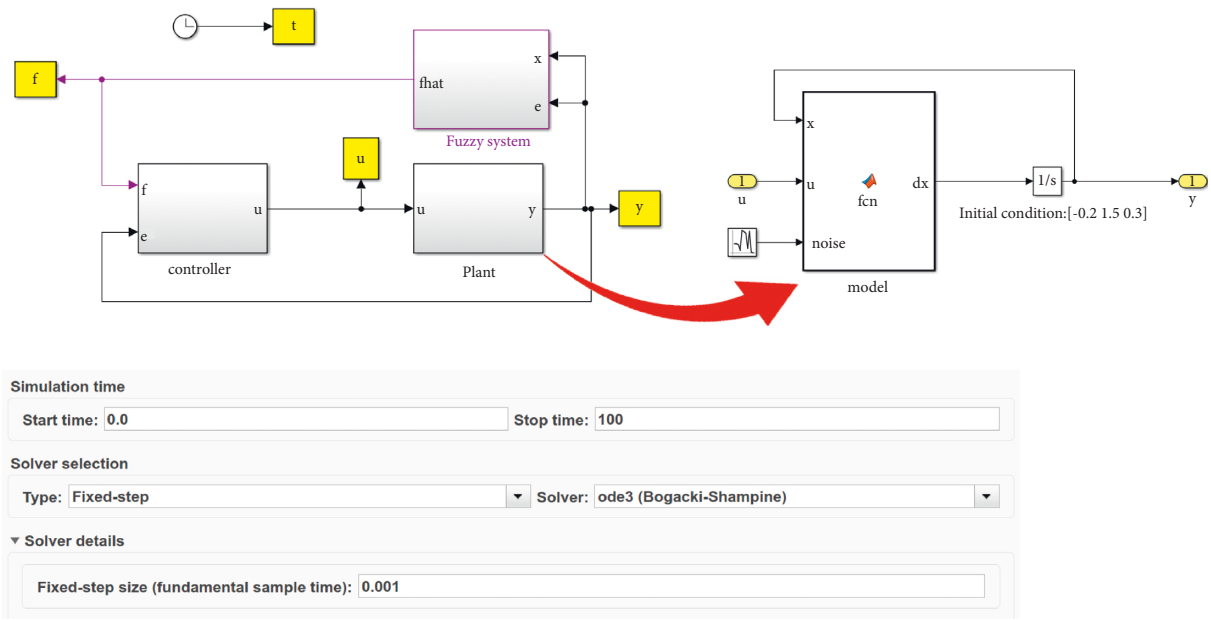

Figure 5: A general view of the simulation scheme.

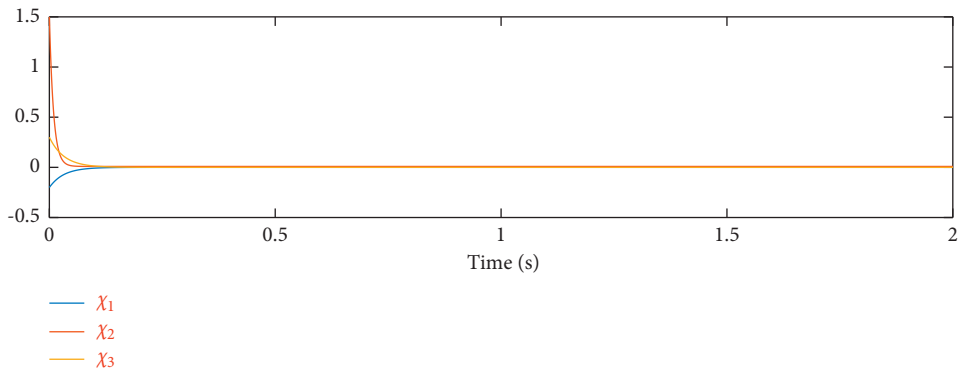

Figure 6: Scenario 6.1: output signals.

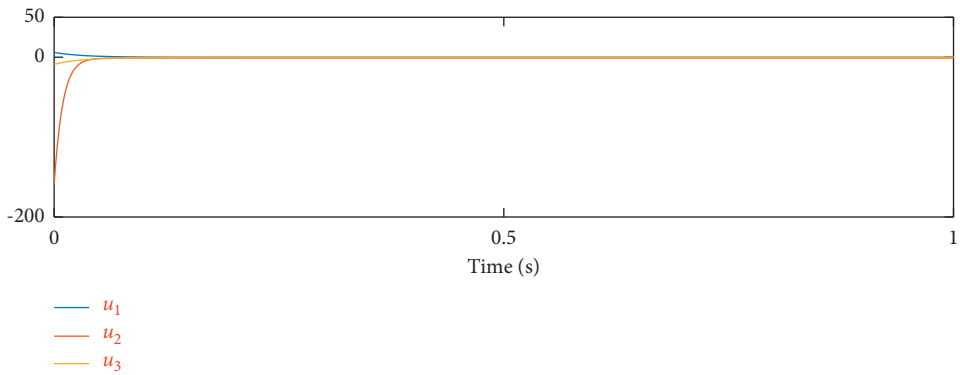

Figure 7: Scenario 6.1: control signals.

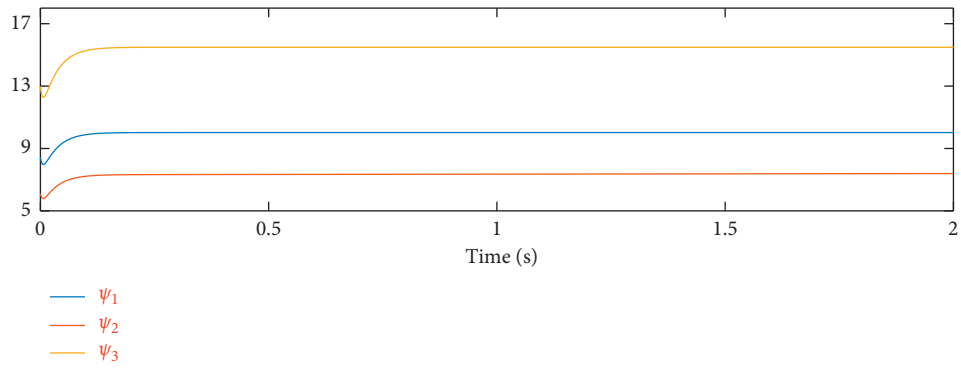

Figure 8: Scenario 6.1: T3-FLS signals.

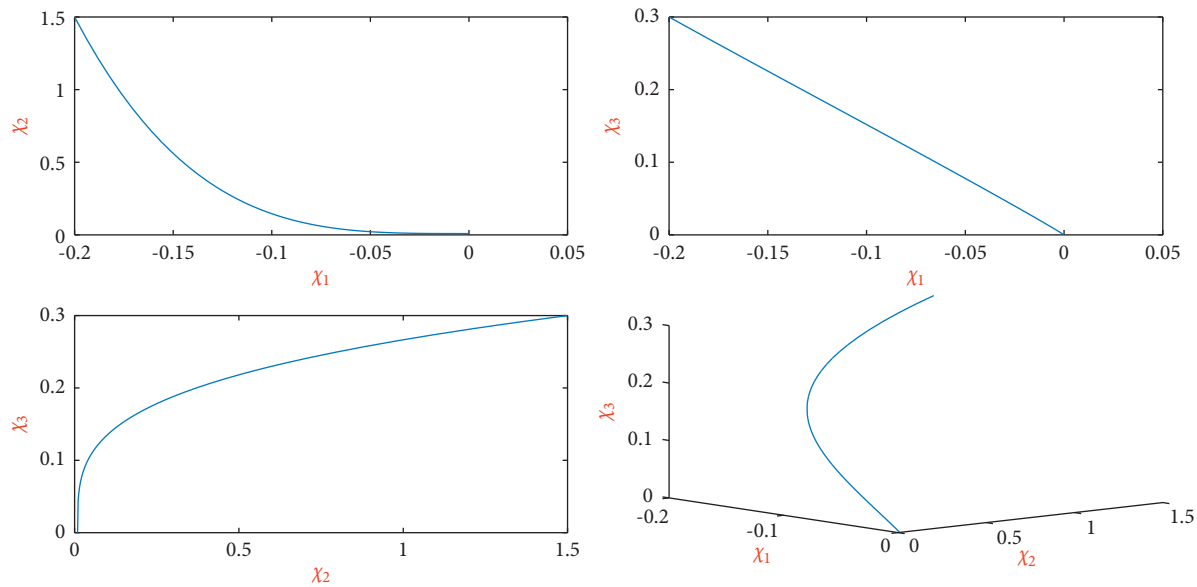

Figure 9: Scenario 6.1: a phase portrait.

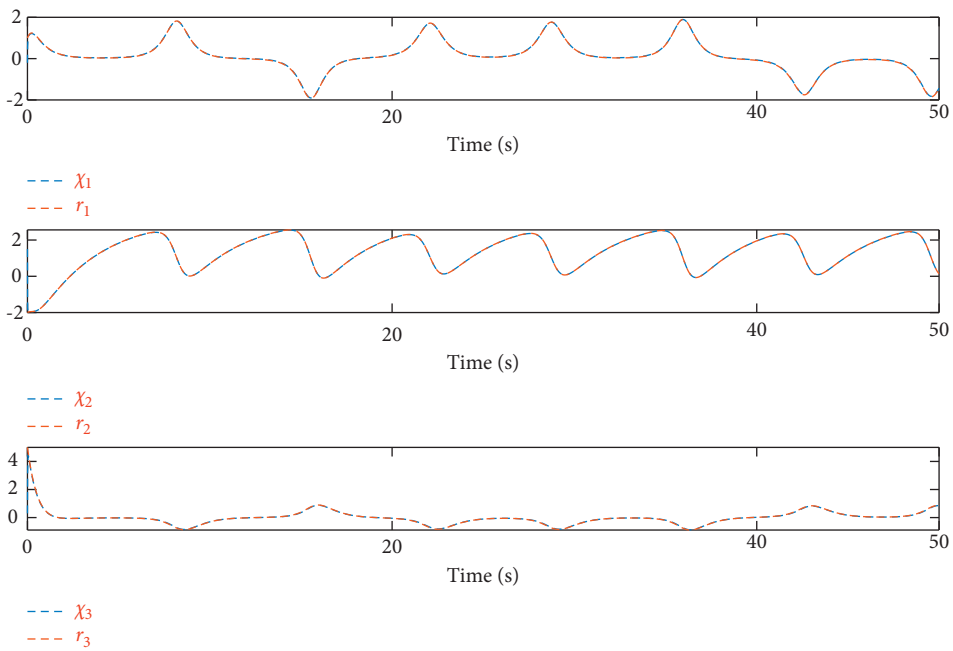

Figure 10: Scenario 6.2: output signals.

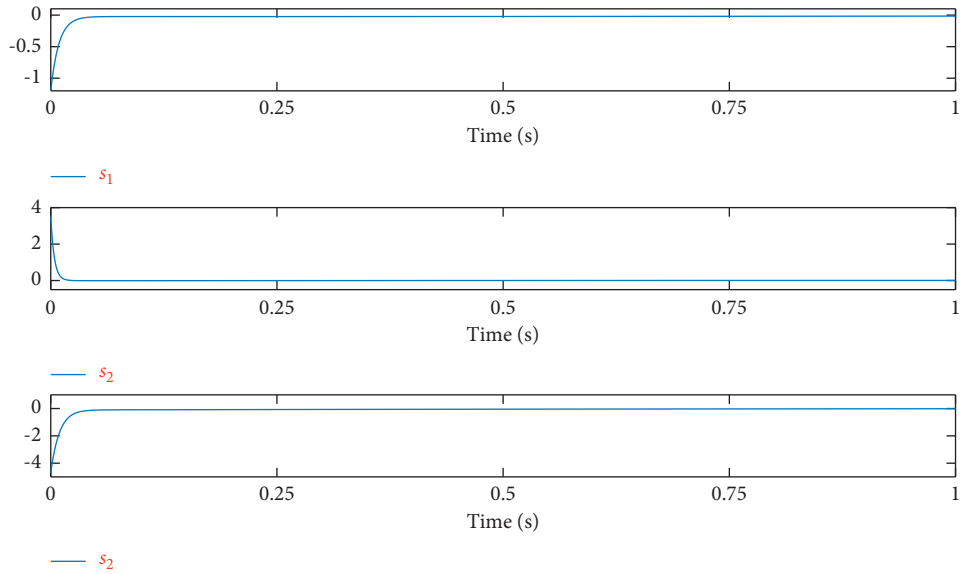

Figure 11: Scenario 6.2: synchronization error signals.

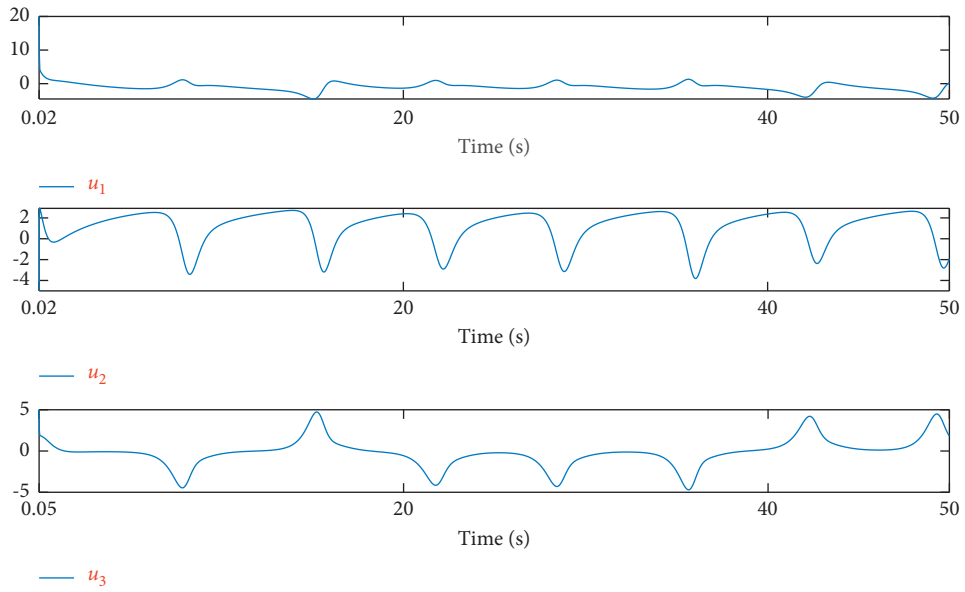

Figure 12: Scenario 6.2: control signals.

To examine the superiority of the suggested control scenario versus other similar approaches, a comparison is presented. The root-mean-square of synchronization errors (RMSEs) for the designed controller are compared with those the type-1 FLS-based controller (T1-FLC) [46], type-2 FLS-based controller (T2-FLC) [47], and generalized FLS-based controller (GT2-FLC) [48]. The comparison results are shown in Table 2. We see that the designed controller gives better synchronization accuracy in high noisy conditions.

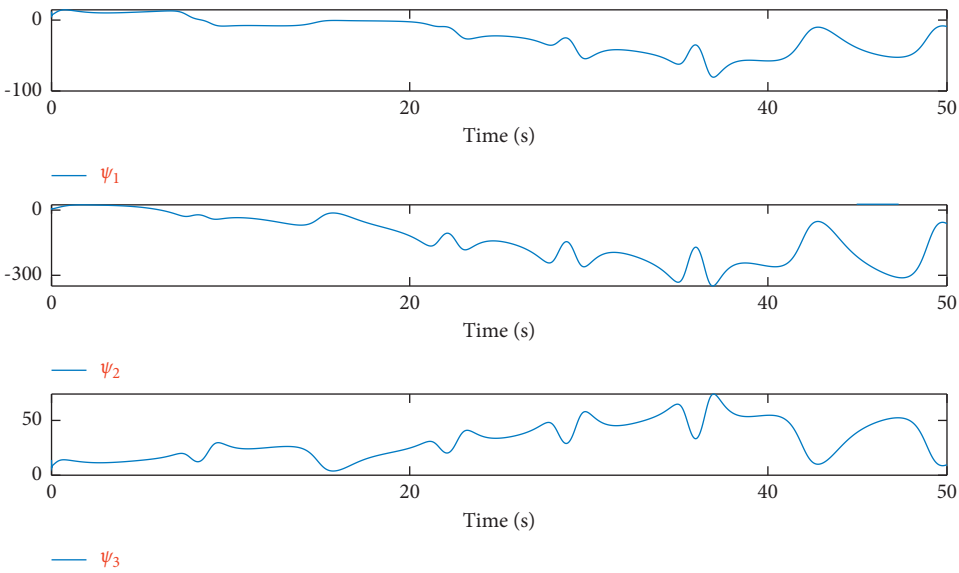

Figure 13: Scenario 6.2: T3-FLS signals.

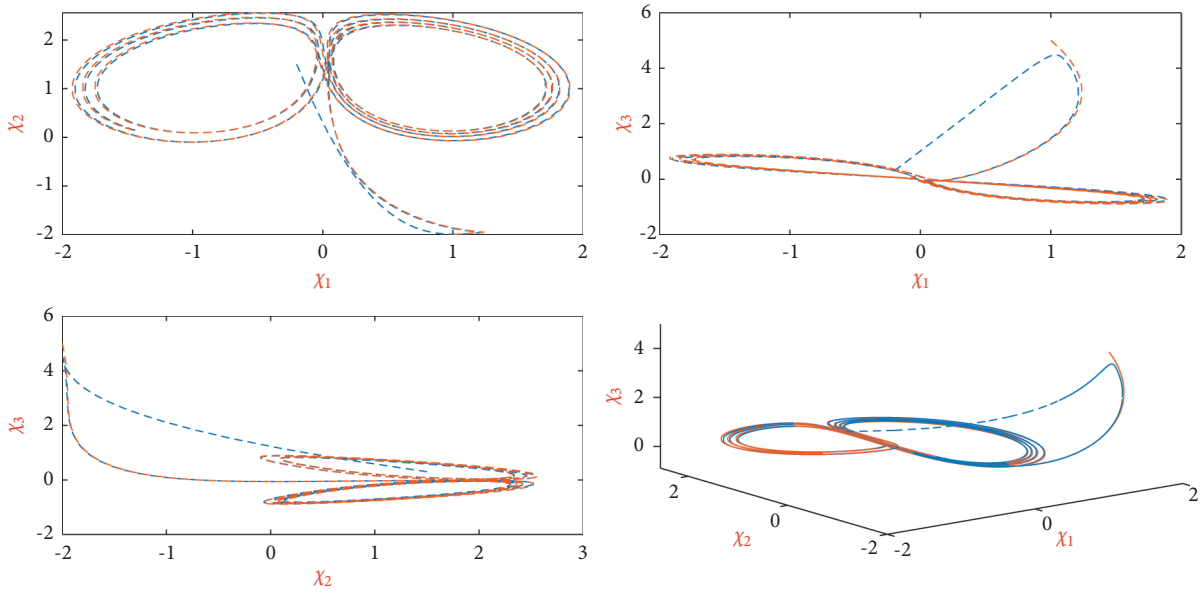

Figure 14: Scenario 6.2: a phase portrait.

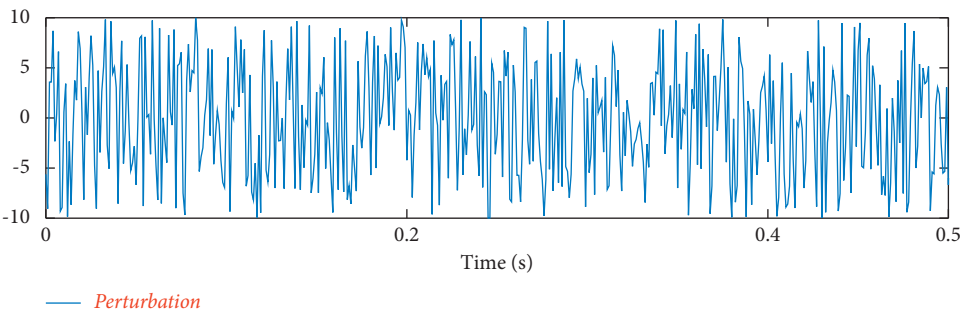

Figure 15: Scenario 6.3: random dynamic perturbation.

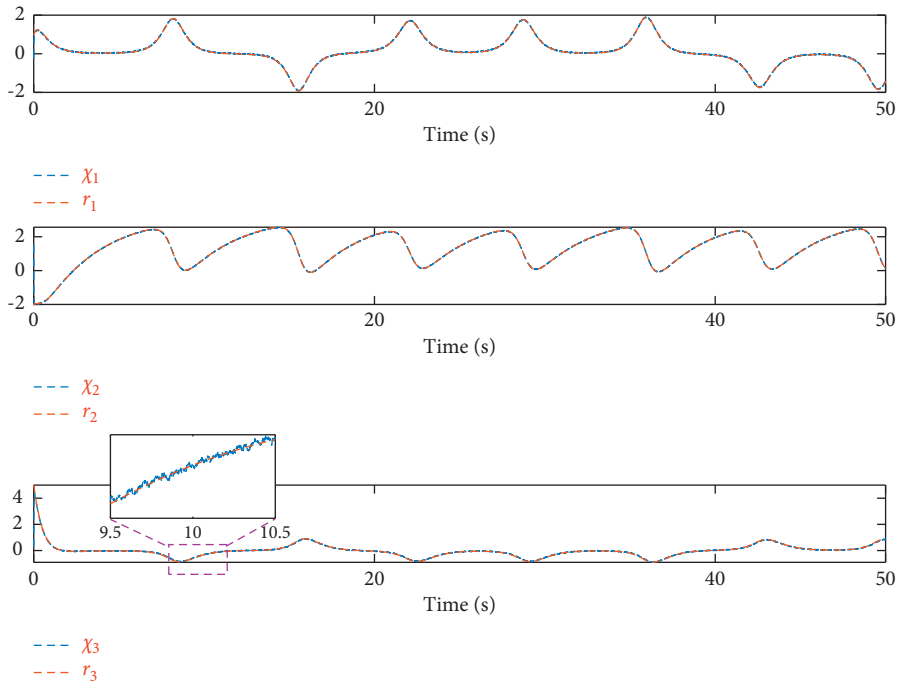

Figure 16: Scenario 6.3: output signals.

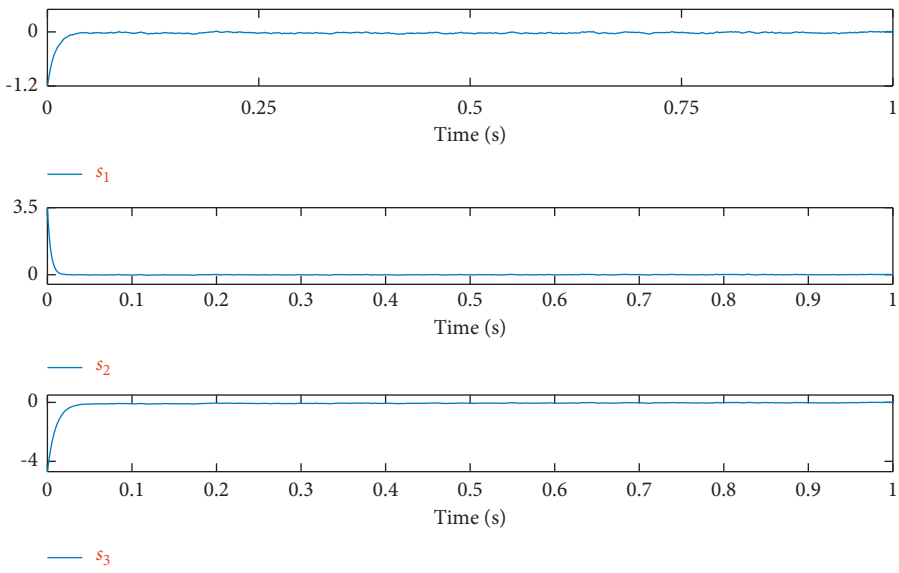

Figure 17: Scenario 6.3: synchronization error signals.

Remark 2. In this paper, a new T3-FLS-based controller is developed for both stabilization and synchronization of financial CSs. The simulations under various conditions show that the designed controller gives the desired efficiency. Even under the high noisy conditions and completely unknown dynamics, it is seen that the presented approach well regulates the target trajectories into reference. Also, by using the designed compensator, the robustness is well preserved under high-level perturbations. The designed controller does not depend on the model of CSs, and then, it can easily be applied to other cases of CSs.

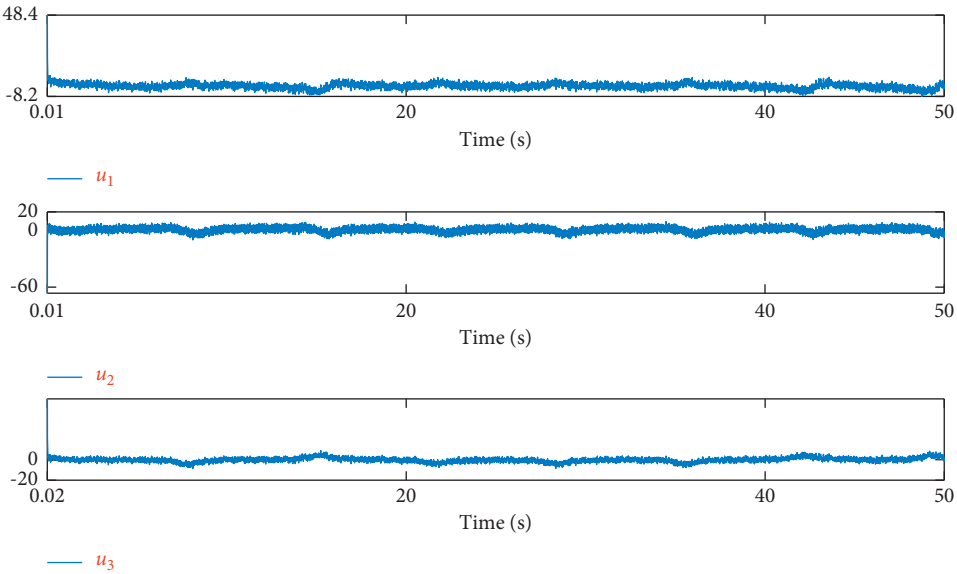

Figure 18: Scenario 6.3: control signals.

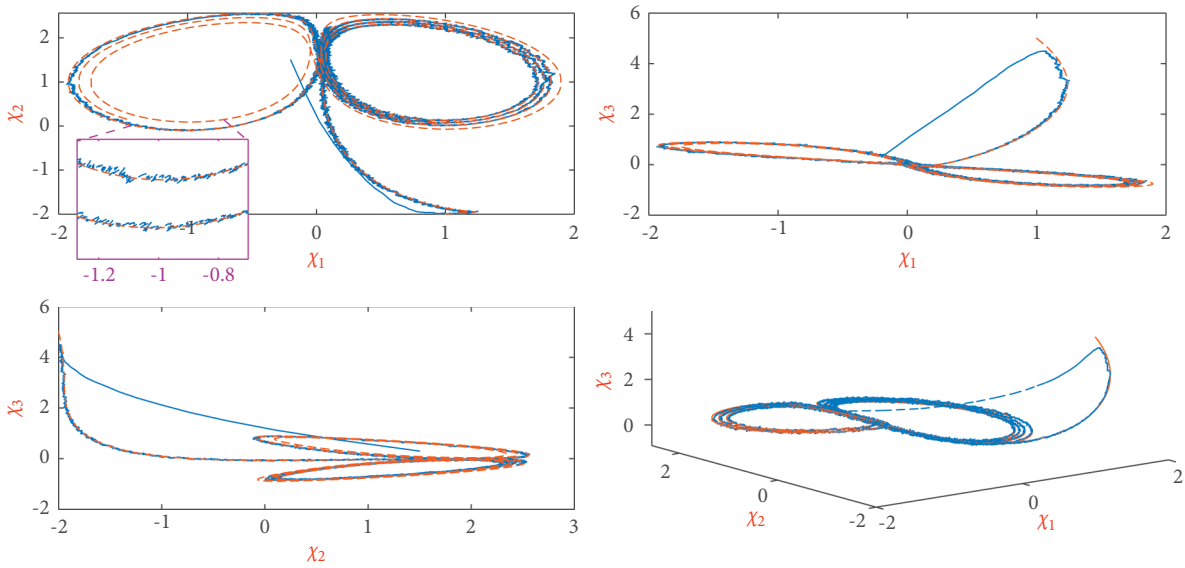

Figure 19: Scenario 6.3: a phase portrait.

Table 2: RMSE comparison.

Method	s_1	s_2	s_3
Proposed	0.0217	0.0266	0.0530
T1-FLC [46]	0.8421	1.0871	1.2820
T2-FLC [47]	0.4023	0.9142	1.0621
GT2-FLC [48]	0.4128	0.8071	1.0278

7. Conclusion

In this paper, the synchronization and stabilization of financial CSs are studied and a new control system is presented. The dynamics is known and is approximated by using the designed T3-FLSs. The robustness is proved through the Lyapunov method. The accuracy of the designed controller is examined in three cases. In the first examination, the stabilization performance is investigated and it shows that all states are perfectly converged to zero at a finite time. For the second examination, the suggested controller is applied for a synchronization problem and it is shown that the case study financial chaotic system well tracks a nonidentical chaotic system; the synchronization errors have

reached zero. For the last examination, the accuracy is evaluated under a high-level noisy condition and it is shown that the suggested control scenario gives perfect results in the presence of high dynamic perturbations and unknown dynamics.

Data Availability

The data that support the findings of this study are available within the article.

Conflicts of Interest

The authors declare that they have no conflicts of interest.

Acknowledgments

This work was supported by the Taif University Researchers Supporting Project grant number (TURSP-2020/266), of Taif University, Taif, Saudi Arabia.

References

[1] H. Zhu, J. Ge, W. Qi, X. Zhang, and X. Lu, "Dynamic analysis and image encryption application of a sinusoidal-polynomial composite chaotic system," *Mathematics and Computers in Simulation*, vol. 198, 2022.

[2] G. Ye, H. Wu, K. Jiao, and D. Mei, "Asymmetric image encryption scheme based on the quantum logistic map and cyclic modulo diffusion," *Mathematical Biosciences and Engineering*, vol. 18, no. 5, pp. 5427–5448, 2021.

[3] A. Musaev and D. Grigoriev, "Analyzing, modeling, and utilizing observation series correlation in capital markets," *Computation*, vol. 9, no. 8, p. 88, 2021.

[4] S. Zhou, Y. Han, L. Sha, and S. Zhu, "A multi-sample particle swarm optimization algorithm based on electric field force," *Mathematical Biosciences and Engineering*, vol. 18, no. 6, pp. 7464–7489, 2021.

[5] D. An, J. Lu, S. Zhang, Y. Li, and A. M. Lopes, "A novel selective encryption method based on skin lesion detection," *Mathematical Problems in Engineering*, vol. 2020, Article ID 7982192, 13 pages, 2020.

[6] A. Anees and I. Hussain, "A novel method to identify initial values of chaotic maps in cybersecurity," *Symmetry*, vol. 11, no. 2, p. 140, 2019.

[7] H. Takhi, K. Kemih, L. Moysis, and C. Volos, "Passivity based sliding mode control and synchronization of a perturbed uncertain unified chaotic system," *Mathematics and Computers in Simulation*, vol. 181, pp. 150–169, 2021.

[8] A. T. Azar, F. E. Serrano, Q. Zhu et al., "Robust stabilization and synchronization of a novel chaotic system with input saturation constraints," *Entropy*, vol. 23, no. 9, p. 1110, 2021.

[9] W. Li, P. Li, and M. Jia, "Chaos control and chaos synchronization of a multi-wing chaotic system and its application in multi-frequency weak signal detection," *AIP Advances*, vol. 11, no. 9, Article ID 095003, 2021.

[10] S. Mobayen, A. Fekih, S. Vaidyanathan, and A. Sambas, "Chameleon chaotic systems with quadratic nonlinearities: an adaptive finite-time sliding mode control approach and circuit simulation," *IEEE Access*, vol. 9, pp. 64558–64573, 2021.

[11] H. Tian, Z. Wang, P. Zhang, M. Chen, and Y. Wang, "Dynamic analysis and robust control of a chaotic system with hidden attractor," *Complexity*, vol. 202111 pages, Article ID 8865522, 2021.

[12] S. Emiroglu, A. Akgül, Y. Adıyaman, T. E. Gümüş, Y. Uyaroglu, and M. A. Yalçın, "A new hyperchaotic system from t chaotic system: dynamical analysis, circuit implementation, control and synchronization," *Circuit World*, vol. 48, no. 2, pp. 265–277, 2021.

[13] M. Dutta and B. K. Roy, "A new memductance-based fractional-order chaotic system and its fixed-time synchronisation," *Chaos, Solitons & Fractals*, vol. 145, Article ID 110782, 2021.

[14] P. Ramesh, M. Sambath, and K. Balachandran, "Hopf bifurcation and synchronisation of a fractional-order butterfly-fish chaotic system," *Journal of Control and Decision*, vol. 9, pp. 117–128, 2021.

[15] I. Ahmad, "A lyapunov-based direct adaptive controller for the suppression and synchronization of a perturbed nuclear spin generator chaotic system," *Applied Mathematics and Computation*, vol. 395, Article ID 125858, 2021.

[16] J. He, F. Chen, and T. Lei, "Fractional matrix and inverse matrix projective synchronization methods for synchronizing the disturbed fractional-order hyperchaotic system," *Mathematical Methods in the Applied Sciences*, vol. 41, no. 16, pp. 6907–6920, 2018.

[17] R. Wang, C. Li, S. Çiçek, K. Rajagopal, and X. Zhang, "A memristive hyperjerk chaotic system: amplitude control, fpga design, and prediction with artificial neural network," *Complexity*, vol. 2021, Article ID 6636813, 17 pages, 2021.

[18] D. Xu, Y. Liu, and M. Liu, "Finite-time synchronization of multi-coupling stochastic fuzzy neural networks with mixed delays via feedback control," *Fuzzy Sets and Systems*, vol. 411, pp. 85–104, 2021.

[19] C.-M. Lin, D.-H. Pham, and T.-T. Huynh, "Synchronization of chaotic system using a brain-imitated neural network controller and its applications for secure communications," *IEEE Access*, vol. 9, pp. 75923–75944, 2021.

[20] M. Zheng, S. Yang, and L. Li, "Aperiodic sampled-data control for chaotic system based on takagi–sugeno fuzzy model," *Complexity*, vol. 2021, pp. 1–8, Article ID 6401231, 2021.

[21] J. Fei, Z. Wang, X. Liang, Z. Feng, and Y. Xue, "Fractional sliding mode control for micro gyroscope based on multilayer recurrent fuzzy neural network," *IEEE Transactions on Fuzzy Systems*, vol. 1, 2021.

[22] M. Dalir and N. Bigdeli, "An adaptive neuro-fuzzy backstepping sliding mode controller for finite time stabilization of fractional-order uncertain chaotic systems with time-varying delays," *International Journal of Machine Learning and Cybernetics*, vol. 12, no. 7, pp. 1949–1971, 2021.

[23] N. Eqra, R. Vatankhah, and M. Eghtesad, "A novel adaptive multi-critic based separated-states neuro-fuzzy controller: architecture and application to chaos control," *ISA Transactions*, vol. 111, pp. 57–70, 2021.

[24] S.-Y. Wang, C.-M. Lin, and C.-H. Li, "Design of adaptive tsk fuzzy self-organizing recurrent cerebellar model articulation controller for chaotic systems control," *Applied Sciences*, vol. 11, no. 4, p. 1567, 2021.

[25] Y. N. Golouje and S. M. Abtahi, "Chaotic dynamics of the vertical model in vehicles and chaos control of active suspension system via the fuzzy fast terminal sliding mode control," *Journal of Mechanical Science and Technology*, vol. 35, no. 1, pp. 31–43, 2021.

[26] C. Urrea, J. Kern, and J. Alvarado, "Design and evaluation of a new fuzzy control algorithm applied to a manipulator robot," *Applied Sciences*, vol. 10, no. 21, p. 7482, 2020.

[27] C. Urrea, J. Kern, and R. López-Escobar, "Design and implementation of a fault-tolerant system for industrial robots under hostile operating conditions," *Computers & Electrical Engineering*, vol. 90, Article ID 106951, 2021.

[28] X. Lu, "A financial chaotic system control method based on intermittent controller," *Mathematical Problems in Engineering*, vol. 2020, Article ID 5810707, 12 pages, 2020.

[29] M.-W. Tian, L. Wang, S.-R. Yan, X.-X. Tian, Z.-Q. Liu, and J. J. P. C. Rodrigues, "Research on financial technology innovation and application based on 5g network," *IEEE Access*, vol. 7, pp. 138614–138623, 2019.

[30] P. Y. Dousseh, C. Ainamon, C. H. Miwadinou, A. V. Monwanou, and J. B. Chabi Orou, "Adaptive control of a new chaotic financial system with integer order and fractional order and its identical adaptive synchronization," *Mathematical Problems in Engineering*, vol. 2021, Article ID 5512094, 15 pages, 2021.

[31] J. Wang and C. Yang, "Chaos synchronization of a finance chaotic system with an integral sliding mode controller," *Journal of Mathematics*, vol. 2021, Article ID 6611031, 9 pages, 2021.

[32] Y.-L. Wang, H. Jahanshahi, S. Bekiros, F. Bezzina, Y.-M. Chu, and A. A. Aly, "Deep recurrent neural networks with finite-time terminal sliding mode control for a chaotic fractional-order financial system with market confidence," *Chaos, Solitons & Fractals*, vol. 146, Article ID 110881, 2021.

[33] S. Bekiros, H. Jahanshahi, F. Bezzina, and A. A. Aly, "A novel fuzzy mixed H2/H optimal controller for hyperchaotic financial systems, Chaos," *Solitons & Fractals*, vol. 146, Article ID 110878, 2021.

[34] Y. Wang, "Research on supply chain financial risk assessment based on blockchain and fuzzy neural networks," *Wireless Communications and Mobile Computing*, vol. 2021, Article ID 5565980, 8 pages, 2021.

[35] J. Wang and R. Lee, "Chaotic recurrent neural networks for financial forecast," *American Journal of Neural Networks and Applications*, vol. 7, no. 1, pp. 7–14, 2021.

[36] X. Zhao, Z. Zhan, and J. Chen, "Adaptive finite time control for a class of hyperchaotic financial systems," *International Journal of Dynamics and Control*, vol. 37, pp. 1–7, 2021.

[37] H. Zhang, "Fuzzy adaptive control of uncertain mimo chaotic systems with unknown control direction," *Complexity*, vol. 2021, Article ID 9914288, 9 pages, 2021.

[38] W. K. Mashwani, H. Shah, M. Kaur, M. A. Bakar, and M. Miftahuddin, "Large-scale bound constrained optimization based on hybrid teaching learning optimization algorithm," *Alexandria Engineering Journal*, vol. 60, no. 6, pp. 6013–6033, 2021.

[39] A. Mohammadzadeh, O. Castillo, S. S. Band, and A. Mosavi, "A novel fractional-order multiple-model type-3 fuzzy control for nonlinear systems with unmodeled dynamics," *International Journal of Fuzzy Systems*, vol. 23, no. 6, pp. 1633–1651, 2021.

[40] R. H. Vafaie, A. Mohammadzadeh, and M. J. Piran, "A new type-3 fuzzy predictive controller for mems gyroscopes," *Nonlinear Dynamics*, vol. 106, no. 1, pp. 381–403, 2021.

[41] M. A. Balootaki, H. Rahmani, H. Moeinkhah, and A. Mohammadzadeh, "Non-singleton fuzzy control for multi-synchronization of chaotic systems," *Applied Soft Computing*, vol. 99, Article ID 106924, 2021.

[42] H. Tirandaz, S. S. Aminabadi, and H. Tavakoli, "Chaos synchronization and parameter identification of a finance chaotic system with unknown parameters, a linear feedback controller," *Alexandria Engineering Journal*, vol. 57, no. 3, pp. 1519–1524, 2018.

[43] M. Jun-hai and C. Yu-Shu, "Study for the bifurcation topological structure and the global complicated character of a kind of nonlinear finance system (i)," *Applied Mathematics and Mechanics*, vol. 22, no. 11, pp. 1240–1251, 2001.

[44] X. Zhao, Z. Li, and S. Li, "Synchronization of a chaotic finance system," *Applied Mathematics and Computation*, vol. 217, no. 13, pp. 6031–6039, 2011.

[45] A. Mohammadzadeh, M. H. Sabzalian, and W. Zhang, "An interval type-3 fuzzy system and a new online fractional-order learning algorithm: theory and practice," *IEEE Transactions on Fuzzy Systems*, vol. 28, no. 9, pp. 1940–1950, 2020.

[46] A. Sambas, S. He, H. Liu, S. Vaidyanathan, Y. Hidayat, and J. Saputra, "Dynamical analysis and adaptive fuzzy control for the fractional-order financial risk chaotic system," *Advances in Difference Equations*, vol. 674, no. 1, pp. 1–12, 2020.

[47] S. Wang, S. Bekiros, A. Yousefpour, S. He, O. Castillo, and H. Jahanshahi, "Synchronization of fractional time-delayed financial system using a novel type-2 fuzzy active control method," *Chaos, Solitons & Fractals*, vol. 136, Article ID 109768, 2020.

[48] M. H. Sabzalian, A. Mohammadzadeh, W. Zhang, and K. Jermsittiparsert, "General type-2 fuzzy multi-switching synchronization of fractional-order chaotic systems," *Engineering Applications of Artificial Intelligence*, vol. 100, Article ID 104163, 2021.